Redox States of Well-Defined π-Conjugated Oligothiophenes Functionalized with Poly(benzyl ether) Dendrons

Joke J. Apperloo,[†] René A. J. Janssen,*[,†] Patrick R. L. Malenfant,[‡] Lambertus Groenendaal,[‡] and Jean M. J. Fréchet*[,‡]

Contribution from the Laboratory for Macromolecular and Organic Chemistry, Eindhoven University of Technology, P.O. Box 513, 5600 MB Eindhoven, The Netherlands, and Department of Chemistry, University of California, Berkeley, California 94720-1460

Received December 3, 1999

Abstract: The redox states of a series of well-defined hybrid dendrimers based on oligothiophene cores and poly(benzyl ether) dendrons have been studied using cyclic voltammetry and variable-temperature UV/visible/near-IR spectroscopy. The oxidation potentials and the electronic transitions of the neutral, singly oxidized, and doubly oxidized states of these novel hybrid materials have been determined as a function of oligothiophene conjugation length varying between 4 and 17 repeat units. The attachment of poly(benzyl ether) dendritic wedges at the termini of these lengthy oligothiophenes considerably enhances their solubility, thus enabling the first detailed investigation of the electronic structure of oligothiophenes having 11 and 17 repeat units with minimal β-substitution. In the case of the undecamer and heptadecamer, we find that the dicationic state consists of two individual polarons, rather than a single bipolaron. The effect of the dendritic poly(benzyl ether) solubilizers on the properties of the redox states varies with the oligothiophene length and dendron size. More specifically, we observe a kinetic limit to the electrochemical oxidation of the oligothiophene core when the dendron is large compared to the electrophore. Finally, we have observed the first example of self-complexation of cation radicals via π-dimerization leading to the formation of dendritic supramolecular assemblies.

Introduction

The functional properties of semiconducting conjugated polymers result from the interplay between the intrinsic features of the polymer chains and interchain interactions. The extent of this interplay will ultimately dictate the role that a semiconducting polymer can play as the active element in new generations of light-emitting diodes, field-effect transistors, and photovoltaic devices.[1] In this regard, dendrimer chemistry[2] may be used as a tool to modify and control interchain interactions and achieve supramolecular ordering of conjugated polymer chains in solid films. Different avenues to combine dendritic architectures and conjugated materials have been proposed in recent years. In one approach, dendrimers were used as a core onto which conjugated oligomers or polymer chains were attached as electroactive and photoactive end groups.[3] Alternatively, dendritic wedges[4] have been used as side chains to solubilize[5a] and segregate the conjugated polymer chain[5] or as end-groups at the termini of well-defined conjugated oligomers to create block copolymer-like architectures.[6−9]

The use of block copolymers with conjugated segments is an emerging area of research in which the repulsive and attractive interactions of the different blocks lead to self-organization of functional polymeric materials on the nanometer scale.[10−12] Dendrimer size and functionality as well as the controllable length of the conjugated segment[13] are well-defined parameters that may be used to manipulate the morphology of block copolymers in a rational way. Furthermore, by controlling the nature of the end-groups of the dendrimers, it is possible to

[†] Eindhoven University of Technology. E-mail: R.A.J.Janssen@tue.nl.
[‡] University of California, Berkeley. E-mail: Frechet@cchem.berkeley.edu.

(1) (a) *Handbook of Organic Conductive Molecules and Polymers*; Nalwa, H. S., Ed.; Wiley: New York, 1997; Vols. 1−4. (b) *Handbook of Conducting Polymers*, 2nd ed.; Skotheim, T. A., Elsenbaumer, R. L., Reynolds, J. R., Eds.; Marcel Dekker: New York, 1998. (c) Dimitrakopoulos, C. D.; Purushothaman, S.; Kymissis, J.; Callegari, A.; Shaw, J. M. *Science* **1999**, *283*, 822.

(2) (a) *Dendritic Molecules: Concepts, Synthesis, Perspectives*; Newkome, G. R., Moorefield, C. N., Vögtle, F., Eds.; VCH: Weinhein, New York, 1996. (b) Tomalia, D. A.; Naylor, A. M.; Goddard, W. A. *Angew. Chem., Int. Ed. Engl.* **1990**, *29*, 138. (c) Fréchet, J. M. J. *Science* **1994**, *263*, 1710. (d) Emrick, T. E.; Fréchet, J. M. J. *Curr. Opin. Colloid Interface Sci.* **1999**, *4*, 15.

(3) (a) Wang, F.; Rauh, R. D.; Rose, T. L. *J. Am. Chem. Soc.* **1997**, *119*, 11106. (b) Miller, L. L.; Kunugi, Y.; Canavesi, A.; Rigaut, S.; Moorefield, C. N.; Newkome, G. R. *Chem. Mater.* **1998**, *10*, 1751. (c) Schenning, A. P. J. H.; Peeters, E.; Meijer, E. W. *J. Am. Chem. Soc.* **2000**. *122*, 4489.

(4) Hawker, C. J.; Fréchet, J. M. J. *J. Am. Chem. Soc.* **1990**, *112*, 7638.

(5) (a) Malenfant, P. R. L.; Fréchet, J. M. J. *Macromolecules* **2000**, *33*, 3634. (b) Karakaya, B.; Claussen, W.; Gessler, K.; Saenger, W.; Schlüter, A.-D. *J. Am. Chem. Soc.* **1997**, *119*, 3296. (c) Bao, Z.; Amundson, K. R.; Lovinger, A. J. *Macromolecules* **1998**, *31*, 8647. (d) Schenning, A. P. J. H.; Martin, R. E.; Ito, M.; Diederich, F.; Boudon, C.; Gisselbrecht, J.-P.; Gross, M. *Chem. Commun.* **1998**, 1013.

(6) Jestin, I.; Levillain, E.; Roncali, J. *Chem. Commun.* **1998**, 2655.

(7) Klaerner, G.; Miller, R. D.; Hawker, C. J. *Polym. Prepr.* **1998**, *39*, 1006.

(8) (a) Malenfant, P. R. L.; Groenendaal, L.; Fréchet, J. M. J. *J. Am. Chem. Soc.* **1998**, *120*, 10990. (b) Malenfant, P. R. L.; Jayaraman, M.; Fréchet, J. M. J. *Chem. Mater.* **1999**, *11*, 3420.

(9) Miller, L. L.; Zinger, B.; Schlechte, J. S. *Chem. Mater.* **1999**, *11*, 2313.

(10) Ruokolainen, J.; Mäkinen, R.; Torkkeli, M.; Mäkelä, T.; Serimaa, R.; ten Brinke, G.; Ikkala, O. *Science* **1998**, *280*, 557.

(11) Li, W.; Maddux, T.; Yu, L. *Macromolecules* **1996**, *29*, 7329.

(12) Hempenius, M. A.; Langeveld-Voss, B. M. W.; van Haare, J. A. E. H.; Janssen, R. A. J.; Sheiko, S. S.; Spatz, J. P.; Möller, M.; Meijer, E. W. *J. Am. Chem. Soc.* **1998**, *120*, 2798.

(13) Well-defined oligothiophenes have been prepared up to 27 repeat units, see: (a) Nakanishi, H.; Sumi, N.; Aso, Y.; Otsubo, T. *J. Org. Chem.* **1998**, *63*, 8632. (b) Martin, R. E.; Diederich, F. *Angew. Chem., Int. Ed. Engl.* **1999**, *38*, 1350.

10.1021/ja994259x CCC: $19.00
Published on Web 07/07/2000

Chart 1. Molecular Structure of the Oligothiophenes and Abbreviations Used in the Text

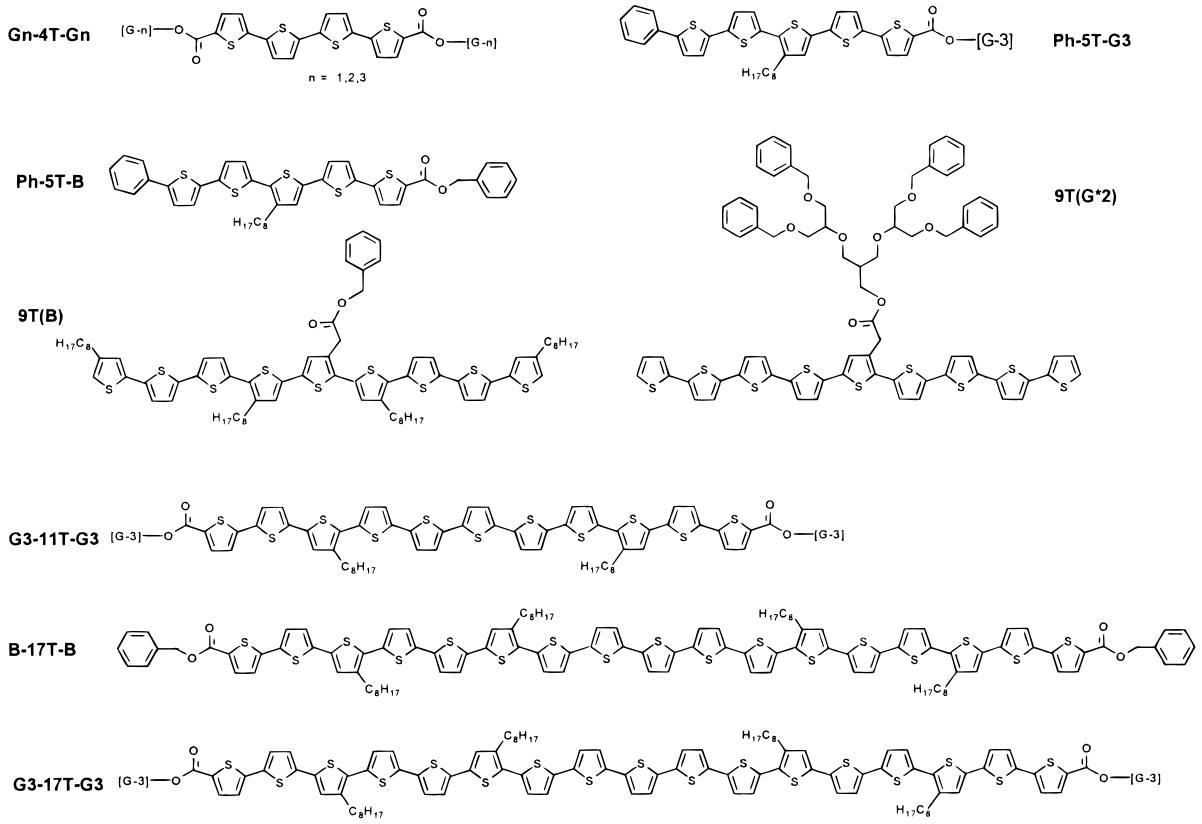

endow these block copolymer architectures with functions such as enhanced adhesion[1414] and energy harvesting,[15] as well as optoelectronic characteristics.[16]

While the incorporation of dendrimers is clearly advantageous with respect to solubility and processability, and they may help provide control over the morphology of thin films, little is known about their influence on the optical and electronic properties of such hybrid materials. The study of these properties has received limited attention so far, and the effect of incorporating dendritic structures on the nature and characteristics of charge carriers has not yet been addressed. Here we present the first detailed investigation of the redox states of well-defined diblock and triblock hybrid dendrimers based on oligothiophene cores and poly(benzyl ether) dendrons (Chart 1), utilizing cyclic voltammetry and variable-temperature UV/visible/near-IR spectroscopy. By incorporating poly(benzyl ether)[4,17] dendrons of different generations (Chart 2) it was possible to investigate the redox states of these systems, i.e. to determine the oxidation potentials as a function of conjugation length, and the evolution of the electronic transitions in the neutral, singly oxidized, and doubly oxidized state. Furthermore, the use of dendrons as solubilizers provides a unique opportunity to study oligothiophenes having minimal β-substitution; such materials would normally be insoluble in the absence of the dendrons. Herein, we show that, in general, poly(benzyl ether) dendritic wedges are compatible with the charges generated in the conjugated oligomers, yet specific "dendrimer related" effects do occur. For instance, depending on their size, the dendritic end groups can affect the kinetics of electrochemical oxidation reactions by sterically preventing the electroactive group from interacting with the electrode. We also present evidence that the presence of bulky G3 poly(benzyl ether) dendrons in diblock materials does not inhibit the well-established π-dimer formation of oligothiophene cation radicals in solution, yet the enthalpy for dimerization is slightly reduced in comparison to the nondendritic analogue. This constitutes the first example in which the π-dimerization of oligothiophene cation radicals is used to construct a supramolecular dendritic assembly. Finally, by

Chart 2. Structure of the First Three Generations of Poly(benzyl ether) Dendrons (**[G-1]-OH**, **[G-2]-OH**, **[G-3]-OH**) Used in the Functionalization of the Oligothiophenes Depicted in Chart 1

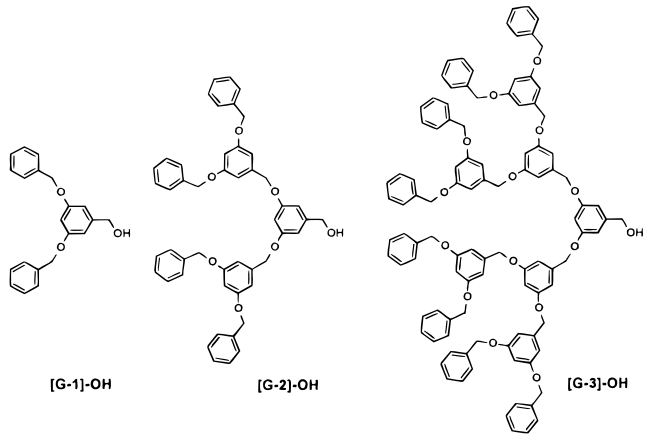

(14) Fréchet, J. M. J.; Gitsov, I.; Monteil, T.; Rochat, S.; Sassi, J. F.; Vergelati, C.; Yu, D. *Chem. Mater*. **1999**, *11*, 1267.

(15) (a) Gilat, S. L.; Adronov, A.; Fréchet J. M. J. *Angew. Chem., Int. Ed.* **1999**, *38*, 1422. (b) Gilat, S. L.; Adronov, A.; Fréchet J. M. J. *J. Org. Chem.* **1999**, *64*, 7474. (c) Adronov, A.; Gilat, S. L.; Fréchet, J. M. J.; Ohta, K.; Neuwahl, F. V. R.; Fleming, G. R. *J. Am. Chem. Soc.* **2000**, *122*, 1175. (d) Adronov, A.; Malenfant, P. R. L.; Fréchet J. M. J. *Chem. Mater.* **2000**, *12*, accepted.

(16) (a) Freeman, A. W.; Fréchet, J. M. J.; Koene, S. C.; Thompson, M. E. *Polym. Prepr.* **1999**, *40*, 1246. (b) Koene, S. C.; Freeman, A. W.; Killeen, K. A.; Fréchet, J. M. J.; Thompson, M. E. *Polym. Mater. Sci. Eng.* **1999**, *80*, 238.

(17) Hawker, C. J.; Fréchet, J. M. J. *J. Chem Soc., Chem. Commun.* **1990**, 1010.

Scheme 1. Synthesis of **G3-17T-G3** Using the Stille Reaction in the Final Step[a]

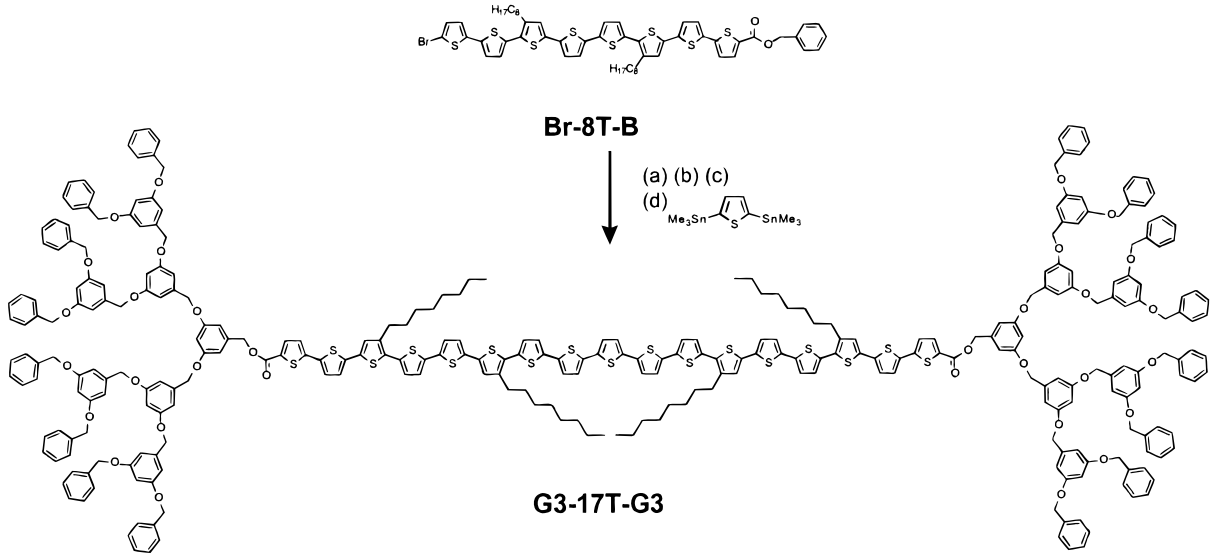

[a] Conditions: (a) KOH (aq)/THF, H_3O^+ (99%); (b) oxalyl chloride, DMF (cat.), CH_2Cl_2 (quant.); (c) **[G-3]-OH**, Py, CH_2Cl_2 (76%); (d) $Pd(PPh_3)_2Cl_2$, DMF, argon (65%).

investigating the oxidized states of the generation three undecamer dumbbell (**G3-11T-G3**) and heptadecamer dumbbell (**G3-17T-G3**), we have been able to characterize the electronic transitions and obtain evidence that, in the doubly oxidized state of long oligothiophenes, two singly charged deformations (also referred to as polarons) are present on the chain, rather than a single, doubly charged, charge carrier (bipolaron). In contrast, for oligomers up to nine units (**9T(B)** and **9T(G*2)**), the dications exhibit typical characteristics of a bipolaron. Hence, these experiments give evidence that a remarkable change in the electronic structure of oligothiophene dications occurs for oligomers with 10 thiophene units. At this point a single (doubly charged) deformation (bipolaron) can dissociate on the chain into two (singly charged) deformations (polarons).

Experimental Section

Commercial grade solvents were purified, dried, and deoxygenated following standard methods. Cyclic voltammograms were recorded in CH_2Cl_2 or CH_3CN with 0.1 M tetrabutylammonium hexafluorophosphate ($TBAPF_6$) as the supporting electrolyte using a Potentioscan Wenking POS73 potentiostat. The working electrode was a platinum disk (0.2 cm^2), the counter electrode was a platinum plate (0.5 cm^2), and a saturated calomel electrode was used as the reference electrode, calibrated against a Fc/Fc^+ couple (+0.470 V vs SCE). The reported oxidation potentials have been obtained with a scan speed of 100 mV/s unless indicated otherwise. UV/visible/near-IR spectra were recorded using a Perkin-Elmer Lambda 900 spectrophotometer equipped with an Oxford Optistat cryostat for variable-temperature experiments. The temperature was kept constant within ± 0.3 K and spectra were corrected for volume changes. The concentrations in the optical experiments varied between 10^{-5} and 10^{-3} M, using both 10 mm and 1 mm near-IR grade suprasil quartz cells. The oxidation experiments were performed by adding small aliquots of a solution of thianthrenium perchlorate ($THIClO_4$)[18] of known concentration in dichloromethane to the solutions of the oligomers from a gas-tight syringe. $THIClO_4$ was chosen as the oxidizing agent because it combines a relatively high oxidation potential with characteristic signals in the UV/visible spectrum ($E = 2.23$ and 4.25 eV).[18,19] The appearance of these signals in the absorption spectra indicates that further addition of $THIClO_4$ does not result in (complete) oxidation of oligothiophene. As an additional advantage, the thianthrene formed in the reduction reaction exhibits an absorption band at $E = 4.83$ eV, well outside the region of interest for the redox states of the present oligothiophenes.

(18) Shine, H. J.; Dais, C. F.; Small, R. *J. Org. Chem.* **1964**, *29*, 21.
(19) Bard, A. J.; Faulkner, L. R. *Electrochemical Methods*; John Wiley and Sons: New York, 1980; p 702.

Results and Discussion

Synthesis. The synthesis and characterization of **G3-11T-G3** and **B-17T-B** have been described previously.[8a] The poly(benzyl ether) dendrons were prepared as described in the literature.[4,17] Triblock compound **G3-17T-G3** was prepared in a multistep process involving the saponification of the α-brominated **Br-8T-B**,[8a] to afford carboxylic acid **Br-8T-COOH**, followed by quantitative conversion to the acid chloride **Br-8T-COCl** using oxalyl chloride in CH_2Cl_2 in the presence of a catalytic amounts of DMF. Reaction of **Br-8T-COCl** with the generation three poly(benzyl ether) dendron having a benzyl alcohol group at the focal point[4,17] in CH_2Cl_2/pyridine afforded **Br-8T-G3**. Finally, a Stille coupling between **Br-8T-G3** and 2,5-bis(trimethylstannyl)thiophene provided **G3-17T-G3** in 65% yield after chromatography (Scheme 1). In contrast to **B-17T-B**, which is slightly soluble in hot CS_2, **G3-17T-G3** is quite soluble in common organic solvents such as THF, $CHCl_3$, and CH_2Cl_2. The **G*n*-4T-G*n*** series ($n = 1$, 2, and 3) was prepared through reaction of the dendritic alcohols with the tetramer diacid chloride **ClCO-4T-COCl**. The latter was obtained via a Stille coupling reaction between methyl 2-bromothiophene-5-carboxylate and 5,5′-(bistrimethylstannyl)-2,2′-bithiophene to provide the symmetric tetramer **Me-4T-Me**. Subsequent saponification with aqueous KOH/THF followed by chlorination with oxalyl chloride provided the diacid chloride **ClCO-4T-COCl** (Scheme 2). While **Me-4T-Me** was rather insoluble, it could be sufficiently purified by trituration in boiling THF. All of the dendritic derivatives where found to be quite soluble in common organic solvents, thus facilitating their handling and purification. The phenyl end-capped pentamer **Ph-5T-B** was prepared via Stille coupling between **Br-5T-B**[8a] and trimethylstannylbenzene. Similarly, **Ph-5T-G3** was prepared by a Stille coupling between **Br-5T-G3**[8a] and trimethylstannylbenzene. Once again, a significant enhancement in solubility is observed upon functionalization of the phenyl end-capped pentamer with a generation three dendron instead of a simple benzyl moiety. Preparation of **9T(B)**[15d] and **9T(G*2)** has been reported elsewhere.[8b]

Scheme 2. Synthesis of **G*n*-4T-G*n*** Triblock Systems[a]

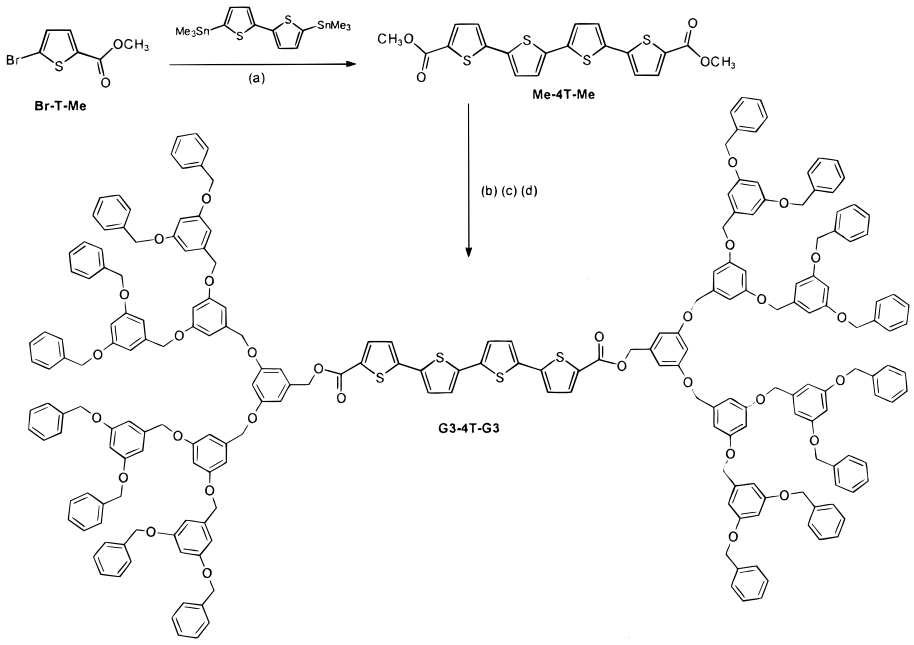

[a] Conditions: (a) $Pd(PPh_3)_2Cl_2$, DMF, argon (81%); (b) $KOH/Me_4NOH{\cdot}THF/H_2O$ (92%); (c) oxalyl chloride, DMF (cat.), CH_2Cl_2 (quant.); (d) **[G-*n*]-OH**, $n = 1$ (55%), 2 (70%), and 3 (60%).

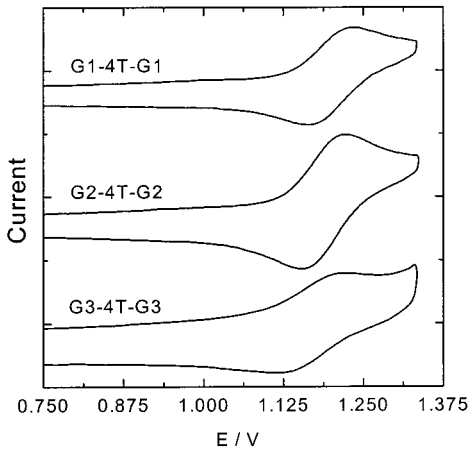

Figure 1. Cyclic voltammograms of **G*n*-4T-G*n*** oligothiophenes, recorded at 295 K in CH_2Cl_2 containing $TBAPF_6$ (0.1 M), scan rate 100 mV/s. Potential vs SCE calibrated against Fc/Fc^+. Curves are offset vertically for clarity.

Singly Oxidized States and π-Dimerization of Short Oligothiophenes ($n \leq 5$) with Poly(benzyl ether) Dendrimer End Groups. First we will address the question whether the electrochemical properties and the nature of the oxidized states of the shorter oligothiophenes ($n \leq 5$) are influenced by the poly(benzyl ether) dendrons.

Figure 1 shows the one-electron oxidation wave at $E^\circ = 1.19$ V vs SCE for **G1-4T-G1**. The oxidation is chemically reversible, which indicates that oxidative polymerization of the 4T moiety does not occur. Clearly, the G1 end groups are effective at inhibiting the coupling of cation radicals via the α-positions, which is a well-known reaction in the one-electron oxidation of short oligothiophenes (*n*Ts with $n < 6$) lacking α-substituents.[20−22] Chemical reversibility is preserved in cycling the potential up to 1.5 V. When the electrochemical potential is further increased a second oxidation wave occurs at $E_{pa} = 1.58$ V. The anodic current associated with the second oxidation wave is considerably larger than that of the first wave, suggesting the transfer of more than one electron. At this point a film is formed on the electrode and subsequent cycles show an increase of current. In a separate experiment we found that the oxidation of the dendritic wedge occurs at $E_{pa1} = 1.57$ V (Table 1) and is completely irreversible. Hence, the $E_{pa} = 1.58$ V wave of **G1-4T-G1** is attributed to the oxidation of the G1 wedge. It must be noted, however, that the second oxidation wave of the quaterthiophene moiety is expected around the same potential and may therefore contribute to the current observed at 1.58 V.

Table 1. Peak Potentials (E_{Pa}), Standard Potentials (E°), and Anodic−Cathodic Peak Separations ($\Delta E_p = |E_{Pa1} - E_{Pc1}|$) for Oxidations of Oligothiophenes Recorded in CH_2Cl_2

compd	E_{pa1} (V)	E_{pa2} (V)	E° (V)	ΔE_p (V)
G1-4T-G1	1.223	1.58	1.190	0.067
G2-4T-G2	1.221	1.58	1.187	0.068
G3-4T-G3	1.225	1.58	1.168	0.115
Ph-5T-B	0.915	1.22	0.884	0.062
Ph-5T-G3	0.905	1.20	0.873	0.065
9T(B)	0.792	0.98	0.772	0.040
9T(G*2)	0.849	1.01	0.807	0.083
G3-11T-G3	0.72			
B-17T-B	0.658			0.210
	0.762[a]			0.225[a]
G3-17T-G3	0.812[a]			0.296[a]
[G-*n*]-OH	1.57			

[a] Measured in CH_3CN.

(20) (a) Hill, M. G.; Mann, K. R.; Miller, L. L.; Penneau, J.-F. *J. Am. Chem. Soc.* **1992**, *114*, 2728. (b) Yu, Y.; Gunic, E.; Zinger, B.; Miller, L. L. *J. Am. Chem. Soc.* **1996**, *118*, 1013. (c) Bäuerle, P.; Segelbacher, U.; Maier, A.; Mehring, M. *J. Am. Chem. Soc.* **1993**, *115*, 10217. (d) Zotti, G.; Schiavon, G.; Berlin, A.; Pagani, G. *Chem. Mater.* **1993**, *5*, 620. (e) Audebert, P.; Hapiot, P.; Pernaut, J.-M.; Garcia P. *J. Electroanal. Chem.***1993**, *361*, 283. (f) Van Haare, J. A. E. H.; Groenendaal, L.; Havinga, E. E.; Janssen, R. A. J.; Meijer, E. W. *Angew. Chem., Int. Ed. Engl.* **1996**, *35*, 638. (g) Sakamoto, A.; Furukawa, Y.; Tasumi, M. *J. Phys. Chem. B* **1997**, *101*, 1726. (h) Apperloo, J. J.; Janssen, R. A. J. *Synth. Met.* **1999**, *101*, 373.

(21) (a) Fichou, D.; Xu, B.; Horowitz, G.; Garnier, F. *Synth. Met.* **1991**, *41−43*, 463. (b) Fichou, D.; Horowitz, G.; Garnier, F. *Synth. Met.* **1990**, *39*, 125. (c) Fichou, D.; Horowitz, G.; Xu, B.; Garnier, F. *Synth. Met.* **1990**, *39*, 243.

(22) Bäuerle, P.; Segelbacher, U.; Gaudl, K.-U.; Huttenlocher, D.; Mehring, M. *Angew. Chem., Int. Ed. Engl.* **1993**, *32*, 76.

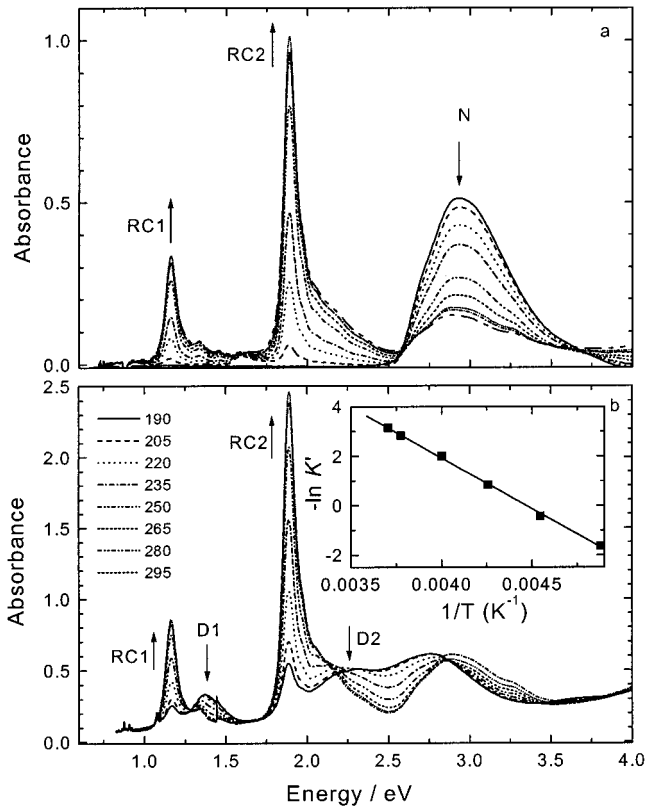

Figure 2. (a) UV/visible/near-IR spectra of **G1-4T-G1** as a function of the doping level by the stepwise addition of 1 equiv of $THIClO_4$ recorded in a 10 mm cell. The graph shows the formation of cation radicals (RC1 and RC2) at the cost of neutral molecules (N). (b) UV/visible/near-IR spectra as a function of temperature (increasing from 180 to 295 K) recorded in a 1 mm cell showing the interconversion from π-dimers (D1 and D2) at low temperatures into cation radicals (RC1 and RC2) at room temperature. The inset shows the variation of the dimerization constant (K', see ref 31) with reciprocal temperature as determined from the increase of the RC2 band in the spectra.

The evolution of the UV/visible/near-IR spectra of **G1-4T-G1** in CH_2Cl_2 solution with progressive oxidation is shown in Figure 2a. Stepwise addition of 1 equiv of $THIClO_4$ results in the gradual formation of **G1-4T-G1**$^{+\bullet}$, which exhibits two characteristic transitions at 1.16 and 1.89 eV (labeled RC1 and RC2, respectively) associated with cation radicals of π-conjugated oligomers.[20−22] The RC1 and RC2 bands are assigned to a dipole-allowed transition from the lowest doubly occupied level to the singly occupied electronic (polaron) level and from the singly occupied level to the lowest unoccupied electronic level, respectively. Bands or shoulders at higher energy, which have a vibronic origin, accompany the two principal bands. The high second oxidation potential of **G1-4T-G1** ($E_{pa2} = 1.58$ V) and the irreversible nature of the second wave preclude the formation of the corresponding dication using $THIClO_4$. Figure 2b shows the reversible changes in the absorption spectra of **G1-4T-G1**$^{+\bullet}$ as a function of temperature. At low temperatures the RC1 and RC2 bands are replaced by new bands at 1.37 (D1) and 2.31 eV (D2). The D1 and D2 bands are hypsochromically shifted with respect to the RC1 and RC2 transitions. This shift is usually observed for π-dimers and is ascribed to a Davydov interaction between the transition dipole moments of the RC1 and RC2 transitions on adjacent radicals in the π-dimer complex.[23] Although the Davydov shift is often observed in the solid state, it is well established that the same phenomenon affects the absorption spectra of dye molecules in solution when these form dimers or aggregates.[24] The low-temperature spectra do not show a charge-transfer transition between the two cation radicals in the π-dimer which is sometimes found at energies below the RC1 band for π-dimers of conjugated oligomer cation radicals.[25,26] In accordance with literature reports on studies of similar systems in solution[20] and X-ray crystallography in the solid state,[27] we propose an interpretation of these effects in terms of π-dimerization, yet it must be noted that σ-dimerization has recently been proposed as an alternative explanation.[28,29] Although there is no unambiguous structural proof whether σ-dimers or π-dimers are formed in solution, we prefer the π-dimer hypothesis. Evidence in favor of π-dimerization is as follows: (1) The *reversible* dimerization of various oligothiophene radical cations reported in the literature so far[20] does not occur preferentially for oligomers with free α-positions, as can be expected for σ-dimerization.[30] (2) The two absorption bands (RC1 and RC2), which are highly characteristic for an *open*-shell conjugated radical ion, are preserved to a large extent in the D1 and D2 bands of the dimer. This strong similarity in electronic structure is not expected for a *closed*-shell σ-dimer. (3) The Davydov model of a face-to-face π-dimer describes qualitatively, and to a large extent quantitatively, the experimentally observed hypsochromic shift of D1 and D2 as compared to RC1 and RC2.[23,24] (4) The dimerization enthalpy generally increases with longer systems,[20] while for σ-dimerization one would expect the opposite behavior.

As a consequence of the negligible spectral overlap and high intensity, the changes in the intensity of the RC2 transition with temperature can be used to estimate the enthalpy of dimerization (ΔH^0_{dim}) by determining the temperature dependence of the equilibrium constant for dimerization (K = [dimer]/[cation radical]^2, see inset of Figure 2b).[31] This analysis gives $\Delta H^0_{dim} = -34$ (±5) kJ/mol for **G1-4T-G1**.

The higher generation dendrimer substituted quaterthiophenes, **G2-4T-G2** and **G3-4T-G3**, show an analogous behavior in cyclic voltammetry and the first one-electron oxidations occur at almost the same potentials as for **G1-4T-G1** (Table 1). However, for **G3-4T-G3** the increase of ΔE_p from 67 to 115 mV reveals that a quasireversible oxidation occurs, indicative of a kinetic limitation to the electron-transfer reaction with increasing size of the dendritic end group. The kinetic limitation for **G3-4T-G3** is supported by the observation that the anodic

(23) π-Dimers and π-stacks in solution have last been reviewed in 1996, see: Miller, L. L.; Mann, K. R. *Acc. Chem. Res.* **1996**, *29*, 417.

(24) Torrance, J. B.; Scott, B. A.; Welber, B.; Kaufman, F. B.; Seiden, P. E. *Phys. Rev. B* **1979**, *19*, 730,and references therein.

(25) Yu, Y.; Gunic, E.; Zinger, B.; Miller, L. L. *J. Am. Chem. Soc.* **1996**, *118*, 1013.

(26) Van Haare, J. A. E. H.; Van Boxtel, M.; Janssen, R. A. J. *Chem. Mater.* **1998**, *10*, 1166.

(27) Graf, D. D.; Duan, R. G.; Campbell, J. P.; Miller, L. L.; Mann, K. R. *J. Am. Chem. Soc.* **1997**, *119*, 5888.

(28) (a) Smie, A.; Heinze, J. *Angew. Chem., Int. Ed. Engl.* **1997**, *36*, 363. (b) Tschuncky, P.; Heinze, J.; Smie, A.; Engelmann, G.; Kossmehl, G. *J. Electroanal. Chem.* **1997**, *433*, 223. (c) Merz, A.; Kronberger, J.; Dunsch, L.; Neudeck, A.; Petr, A.; Parkanyi, L. *Angew. Chem., Int. Ed. Engl.* **1999**, *38*, 1442.

(29) (a) Effenberger, F.; Mack, K.-E.; Niess, R.; Reisinger, F.; Steinbach, A.; Stohrer, W.-D.; Stezowski, J. J.; Rommel, I.; Maier, A. *J. Org. Chem.* **1998**, *53*, 4379−4386. (b) Effenberger, F.; Stohrer, W.-D.; Mack, K.-E.; Reisinger, F.; Steufert, W.; Kramer, H. E. A.; Föll, R.; Vogelmann, E. *J. Am. Chem. Soc.* **1990**, *112*, 4849.

(30) In fact, a recent study on the dimerization of oligothienylenevinylene radical cations reveals a much stronger preference for dimerization of oligomers with α-alkyl substituents than β-substituents; see ref 37.

(31) The normalized absorbance A of the RC2 transition can be used to determine K via the relation $K = (1 - A)/2C_0A^2$), where C_0 is the total concentration of cation radicals (present as free monomers or incorporated in π-dimers). ΔH^0_{dim} can then be obtained from the slope of a plot of ln K vs $1/T$. Alternatively, $K' = KC_0$ can be used to determine ΔH^0_{dim}.

Table 2. Energies of the Electronic Transitions of the Neutral (N), Cation Radical (RC), Dication (DC), and π-Dimers (D) as Well as Redox States of Oligothiophenes and the Enthalpy of Dimerization of Cation Radicals

compd	*N* (eV)	RC1 (eV)	RC2 (eV)	DC1 (eV)	DC2 (eV)	D1 (eV)	D2 (eV)	ΔH^0_{dim} (kJ/mol)
G1-4T-G1	2.93	1.16	1.89	*a*	*a*	1.37	2.32	-34 ± 5
G2-4T-G2	2.93	1.16	1.89	*a*	*a*			*b*
G3-4T-G3	2.93	1.16	1.89	*a*	*a*			*b*
Ph-5T-B	2.86	0.93	1.66	1.27		1.09	1.99	-51 ± 3
Ph-5T-G3	2.85	0.94	1.65	1.31		1.11	2.00	-38 ± 2
9T(B)	2.83	0.63	1.44	0.80	1.62			
9T(G*2)	2.76	0.63	1.47	0.83	1.62			
G3-11T-G3	2.60	0.69	1.42	0.89	1.68			
B-17T-B	2.56	0.77	1.82					
G3-17T-G3	2.59	0.66	1.74	0.75	1.62			

[a] Dication cannot be generated using $THIClO_4$. [b] Low stability inhibited variable-temperature experiments to assess π-dimerization.

peak current (i_{pa}) scales with the scan rate (υ) according to $i_{pa} \sim \upsilon^{0.5}$ for G1 and G2 in the range $\upsilon = 25-200$ mV/s, but as $i_{pa} \sim \upsilon^{0.25}$ for G3. Similar observations have been made with porphyrin core dendrimers.[32,33] It is interesting to note that in a recent study done on dendritic oligothienylenevinylenes both the oxidation potential and electron-transfer kinetics were found to be independent of dendron generation for a system containing five vinylene and four thienylene units (5V4T).[6] The lack of dependence of the electroactivity on dendron generation was attributed to the length of the electrophore that prevents its complete encapsulation by the dendritic structure. The reduced length of 4T in **G*n*-4T-G*n*** (ca. 65%) in comparison to 5V4T might explain the kinetic limitation of electron transfer to the electrode observed in our system.

G2-4T-G2 and **G3-4T-G3** can also be oxidized to the corresponding cation radicals and exhibit similar UV/visible/near-IR spectra as **G1-4T-G1** (Table 2). It would have been interesting to investigate π-dimerization of these cation radicals, to assess a possible generation dependence. Unfortunately, the stability of the **G2-4T-G2**$^{+\bullet}$ and **G3-4T-G3**$^{+\bullet}$ cation radicals is less than that of **G1-4T-G1**$^{+\bullet}$ and samples deteriorated significantly in less than 10 min, thus preventing variable-temperature experiments that typically require 2−3 h. The loss of the RC1 and RC2 bands for **G2-4T-G2**$^{+\bullet}$ and **G3-4T-G3**$^{+\bullet}$ in time is not accompanied by the full recovery of the π−π* absorption of the neutral oligomer. This is a clear indication that the 4T moiety is participating in an irreversible chemical reaction. Since G1 dendritic end groups are effective in stabilizing the otherwise very reactive 4T$^{+\bullet}$ cation radical in **G1-4T-G1**$^{+\bullet}$**,** we rationalize the decreased lifetime of **G2-4T-G2**$^{+\bullet}$ and **G3-4T-G3**$^{+\bullet}$ by an intramolecular reaction of the 4T$^{+\bullet}$ cation radical with back-folded dendritic wedges. Since **G1-4T-G1**$^{+\bullet}$ is expected to exhibit a similar reactivity in intermolecular reactions as the generation two and three isomers, but lacks the possibility of back-folding of the dendritic wedge, we prefer an intramolecular degradation mechanism to explain the reduced stability of **G2-4T-G2**$^{+\bullet}$ and **G3-4T-G3**$^{+\bullet}$, in comparison with **G1-4T-G1**$^{+\bullet}$. We speculate that oxidation of the dendritic wedge ($E_{pa} = 1.58$ V) may provide a radical intermediate that is reactive toward the 4T conjugated system, but we were not able to confirm this experimentally.

The two quinquethiophenes **Ph-5T-B** and **Ph-5T-G3** exhibit two consecutive one-electron chemically reversible oxidation waves at about $E_{pa1} = 0.90$ and $E_{pa2} = 1.20$ V (Table 1, Figure 3). **Ph-5T-B** can be oxidized to the cation radical by adding 1 equiv of $THIClO_4$. The singly oxidized state exhibits two

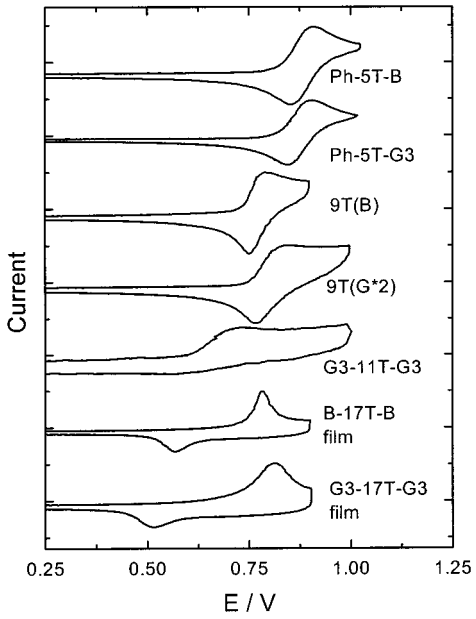

Figure 3. Selected cyclic voltammograms of oligothiophenes shown in Chart 1, recorded at 295 K in CH_2Cl_2 containing $TBAPF_6$ (0.1 M), scan rate 100 mV/s. Potential vs SCE calibrated against Fc/Fc^+. Curves are offset vertically for clarity.

electronic transitions (RC1 and RC2 at 0.93 and 1.66 eV, respectively) (Figure 4a). Subsequent addition of a second equivalent of $THIClO_4$ produces the dication, which shows a single strong transition at 1.27 eV (Table 2). The cation radical of **Ph-5T-B** is stable on the time scale of several hours, thus allowing the use of variable-temperature UV/visible/near-IR spectroscopy to investigate π-dimerization at low temperatures. Figure 4a shows the changes that occur in the spectrum as the temperature decreases. The RC1 and RC2 bands are reversibly replaced by two new bands attributed to the π-dimer: D1 and D2 at 1.09 and 1.99 eV, respectively. Using the RC2 band as a gauge to determine the equilibrium constant,[31] the enthalpy for π-dimerization was found to be $\Delta H^0_{dim} = -51$ (±3) kJ/mol, which is in good agreement with related systems.[20]

The results of the oxidation experiments on **Ph-5T-G3** are analogous to those of the benzyl ester derivative **Ph-5T-B**. The oxidation is fully reversible to both the cation radical (RC1 = 0.94, RC2 = 1.65 eV) and the dication (DC = 1.31 eV). **Ph-5T-G3**$^{+\bullet}$ also forms π-dimers when the temperature is decreased. The more extended conjugation of **Ph-5T-G3** in comparison with **G3-4T-G3** enhances the intrinsic stability of the corresponding cation radical significantly, thus allowing the heat of dimerization to be measured. Comparison of Figure 4a and Figure 4b shows that the π-dimerization of the dendritic oligothiophene derivative is less pronounced. The reduced

(32) Dandliker, P. J.; Diederich, F.; Zingg, A.; Gisselbrecht, J. P.; Gross, M.; Louati, A.; Sanford, E. *Helv. Chim. Acta* **1997**, *80*, 1773 and references therein.

(33) Pollak, K. W.; Leon, J. W.; Fréchet J. M. J.; Maskus, M.; Abruna, H. D. *Chem. Mater.* **1998**, *10*, 30.

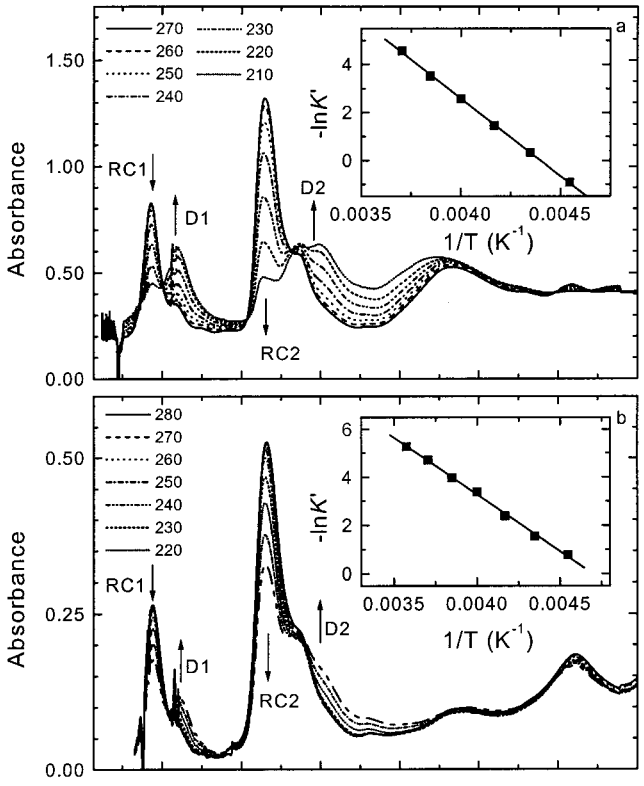

Figure 4. UV/visible/near-IR spectra of (a) **Ph-5T-B**$^{+\bullet}$ as a function of temperature (decreasing from 270 to 210 K) showing the interconversion from cation radicals (RC1 and RC2) at room temperature into π-dimers (D1 and D2) at low temperatures. The inset shows the variation of the dimerization constant (K', see ref 31) with reciprocal temperature as determined from the decrease of the RC2 band in the spectra. (b) **Ph-5T-G3**$^{+\bullet}$ in the temperature range from 280 to 220 K.

tendency to form π-dimers is also reflected in the lower dimerization enthalpy of **Ph-5T-G3**$^{+\bullet}$ which was found to be $\Delta H^0_{\rm dim} = -38\ (\pm 2)$ kJ/mol as compared to $\Delta H^0_{\rm dim} = -51\ (\pm 3)$ kJ/mol for **Ph-5T-B**$^{+\bullet}$. The decreased π-dimerization may be rationalized by an increase in steric interactions between the two cation radicals, but it may also result from a decrease in the solvation of the dendritic wedges when incorporated into a π-dimer. The formation of (**Ph-5T-G3**)$_2^{2+}$ π-dimers is the first example in which the self-complexation of conjugated cation radicals provides a supramolecular dendritic assembly. Although the exact geometry of these assemblies is still unknown, we speculate that the dumbbell shaped dimer depicted in Figure 5 represents a plausible arrangement.

Singly and Doubly Oxidized States of Intermediate Length Oligothiophenes ($n = 9$) with Varying Degrees of Substitution. In this section we address the redox properties of two related nonithiophenes, **9T(B)** and **9T(G*2)**. By introducing the aliphatic ether dendron (**G*2**) it is possible to study an oligomer of unprecedented length, having only a single solubilizing group.

The electrochemical oxidation of **9T(B)** and **9T(G*2)** is chemically reversible when the voltage scans are reversed before $E = 0.9$ and 1.0 V, respectively (Figure 3). Distances between anodic and cathodic peaks are 40 and 83 mV, respectively. Extension of the sweep to higher potentials gives ill-resolved quasireversible broad second oxidation waves at 0.98 and 1.01 V. This complex behavior is analogous to previous results on an alkyl-substituted nonithiophene.[34] At $E = 1.2$ V the oxidation of **9T(G*2)** becomes irreversible and film formation occurs at the electrode as inferred from an increasing current in each subsequent cycle.

The UV/visible/near-IR spectra of **9T(B)** and **9T(G*2)** as a function of doping level are shown in Figure 6, spectra a and b, respectively, and show that both compounds exhibit a very similar behavior. By stepwise addition of 2 equiv of $THIClO_4$ these nonamers can be oxidized to the cation radical and the dication. While the cation radicals of **9T(B)** and **9T(G*2)** exhibit two strong transitions below the optical band gap of the neutral oligomer, the corresponding dications show only one strong subgap transition. Such a single transition for a doubly charged dication is highly characteristic of a bipolaronic charge carrier, i.e. the two charges belong to a single geometric deformation of the chain.[35] Comparing the optical transitions of the redox states of the two nonamers (Table 2) reveals that the $\pi-\pi^*$ transition of neutral **9T(G*2)** is at lower energy than that of **9T(B)**. This is rationalized by the minimal substitution of **9T-(G*2)** which induces a more planar structure and, hence, a longer effective conjugation length. This result is consistent with previous work comparing β-substituted and nonsubstituted oligothiophenes.[36] However, the oxidation potential of **9T(B)** is relatively lower as a consequence of the electron-releasing alkyl groups. Apparently, the electron-releasing effect outweighs the reduction of the conjugation length that results from the inter-ring torsion due to steric hindrance of the alkyl groups, thus lowering the oxidation potential.

The two polaron bands are of almost the same intensity for these 9T derivatives. Figure 6 shows that the DC transition of the dication has developed before the N band of the neutral oligomer has fully disappeared. This is due to the fact that the first two oxidation waves are close in energy, thus giving rise to a disproportionation reaction in which the cation radicals are in equilibrium with a neutral and doubly charged oligomer:

$$2\ n\mathrm{T}^{+\bullet} \rightleftarrows n\mathrm{T} + n\mathrm{T}^{2+}$$

The spectral changes of **9T(B)**$^{+\bullet}$ and **9T(G*2)**$^{+\bullet}$ with temperature revealed a rather complex behavior, which could not be analyzed in detail. Although some indications of π-dimerization were observed, the changes with temperature were relatively small and could also be interpreted in terms of a shift in the disproportionation equilibrium to the neutral and dicationic state as observed recently for thienylenevinylene oligomers.[37]

Singly and Doubly Oxidized States of Long Oligothiophenes ($n \geq 11$) with Poly(benzyl ether) Dendrimer End Groups. The results on **9T(B)** and **9T(G*2)** support the view that open-shell cation radicals (polarons) and closed-shell dications (bipolarons) are the primary redox species in oligothiophenes of limited and intermediate length. The nature of the doubly oxidized state for long oligothiophenes, however, is less clear.[34,38] With the high solubility of the present dendrimer functionalized oligithiophenes, the oxidized states up to the heptadecamer (**G3-17T-G3**) can be analyzed in detail for the first time. The possibility that long oligothiophene dications possess an open-shell structure with two individual polarons has been proposed for an duodecithiophene derivative (12T).[34] Such a transition with increasing chain length can be explained

(34) Van Haare, J. A. E. H.; Havinga, E. E.; Van Dongen, J. L. J.; Janssen, R. A. J.; Cornil, J.; Brédas, J.-L. *Chem. Eur. J.* **1998**, *4*, 1509.

(35) (a) Fesser, K.; Bishop, A. R.; Campbell, D. K. *Phys. Rev. B.* **1983**, *27*, 4804. (b) Cornil, J.; Beljonne, D.; Brédas, J. L. *J. Chem. Phys.* **1995**, *103*, 842.

(36) Horowitz, G.; Yassar, A.; Von Bardeleben, H. J. *Synth. Met.* **1994**, *62*, 245.

(37) Apperloo, J. J.; Raimundo, J.-M.; Frère, P.; Roncali J.; Janssen, R. A. J. *Chem. Eur. J.* **2000**, *6*, 1698.

(38) Nessakh, B.; Horowitz, G.; Garnier, F.; Deloffre, F.; Srivastava, P.; Yassar, A. *J. Electroanal. Chem.* **1995**, *399*, 97.

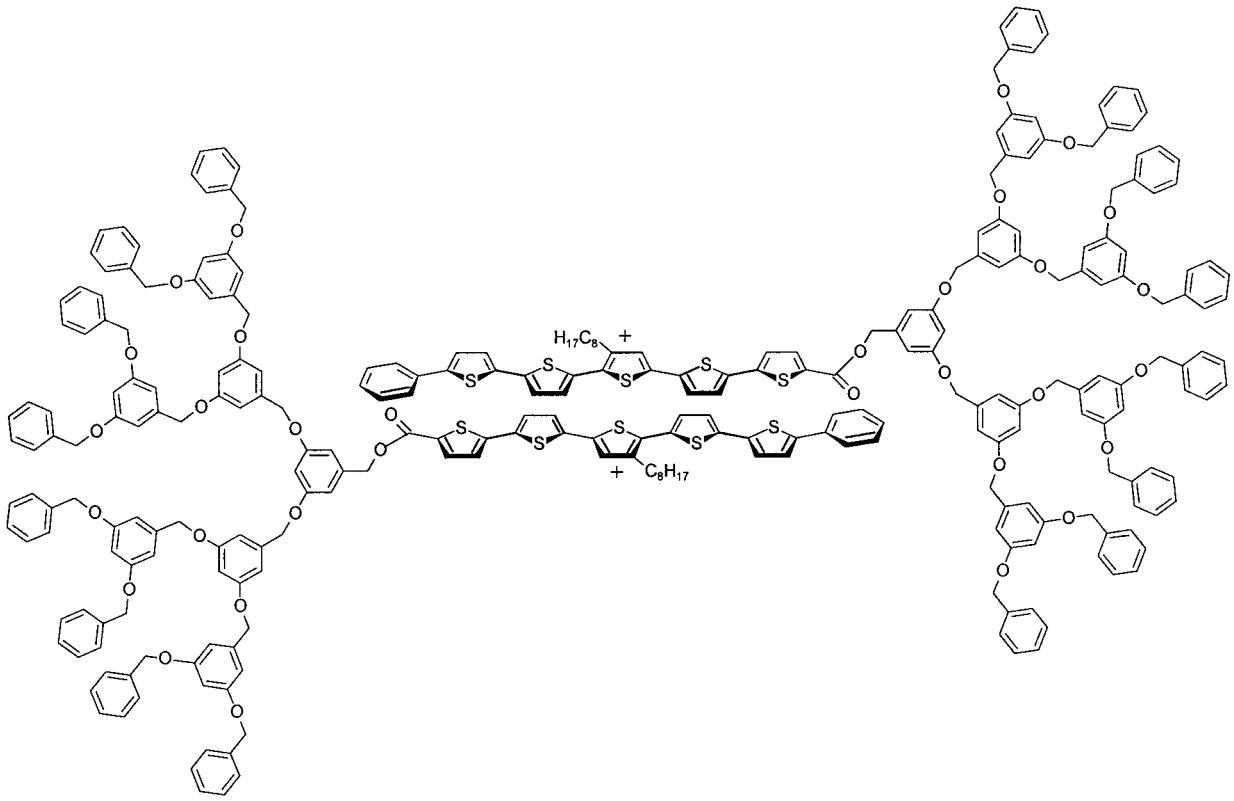

Figure 5. Proposed schematic structure of the dumbbell π-dimer of **Ph-5T-G3**$^{+\bullet}$.

by the fact that the decrease of Coulomb energy obtained by moving the two like charges apart may (at a certain length) outweigh the concurrent energy cost that follows from the fact that the two charges no longer share the same geometrical deformation.

As can be seen in Figure 3 there is a loss of electrochemical reversibility for **G3-11T-G3** in comparison with shorter oligothiophenes. However, repetitive cycling of the voltammogram produces the same curve without the appearance of new peaks. This may be due to a slow electron-transfer reaction with the oligomer.[39]

G3-11T-G3 can be reversibly oxidized to the cation radical and dication via addition of $THIClO_4$. The evolution of the UV/visible/near-IR spectra with increasing doping level is shown in Figure 7. After addition of the first aliquot of $THIClO_4$, the RC1 and RC2 transitions of **G3-11T-G3**$^{+\bullet}$ are found at 0.69 and 1.42 eV, respectively. However, at higher oxidation levels, the two transitions shift more or less continuously to 0.89 and 1.68 eV, when the dication is present. The last spectrum shown in Figure 7 corresponds to the highest degree of oxidation that may be reached with $THIClO_4$. A very similar complex behavior has previously been observed for two other lengthy oligothiophenes (e.g. a polystyrene−undecithiophene−polystyrene triblock copolymer[12] and a tetradodecyl duodecithiophene[34,38]). In both cases the initial spectrum of the cation radical shifts hypsochromically with increasing extent of oxidation. The inset of Figure 7 shows that the spectrum recorded halfway through the oxidation process is temperature independent and demonstrates that the formed redox state has no tendency to dimerize at low temperature.[40] The reason for the complex changes in the UV/visible/near-IR spectra with increasing oxidation is a matter still under debate.[34,38] Although it is well-established that

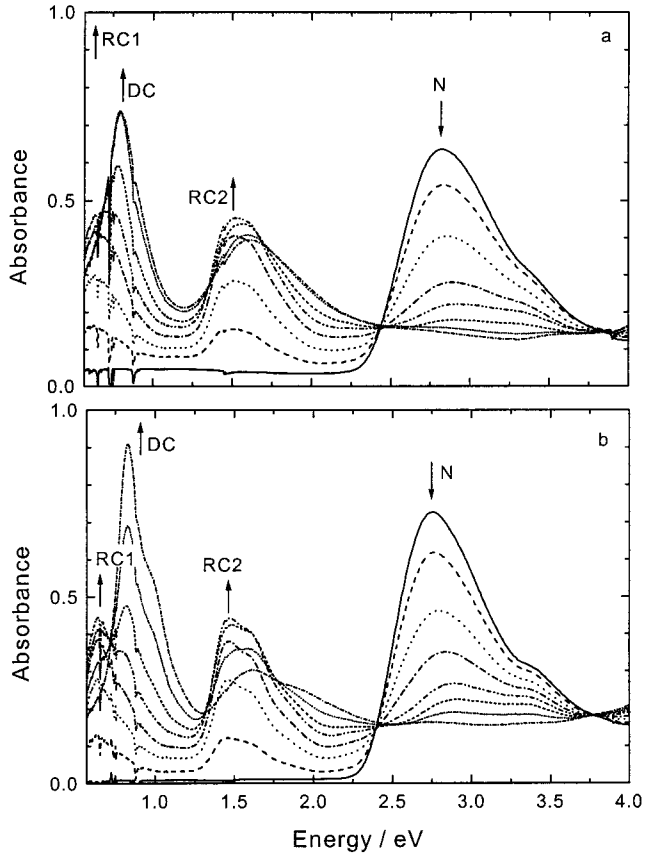

Figure 6. UV/visible/near-IR spectra of (a) **9T(B)** and (b) **9T(G*2)** as a function of the doping level by the stepwise addition of 2 equiv of $THIClO_4$ recorded in a 10 mm cell. The graph shows the formation of cation radicals (RC1 and RC2) at the expense of neutral molecules (N).

(39) *Electroanalytical Chemistry*; Bard, A. J., Ed.; Marcel Dekker: New York, 1986; Vol. 14.

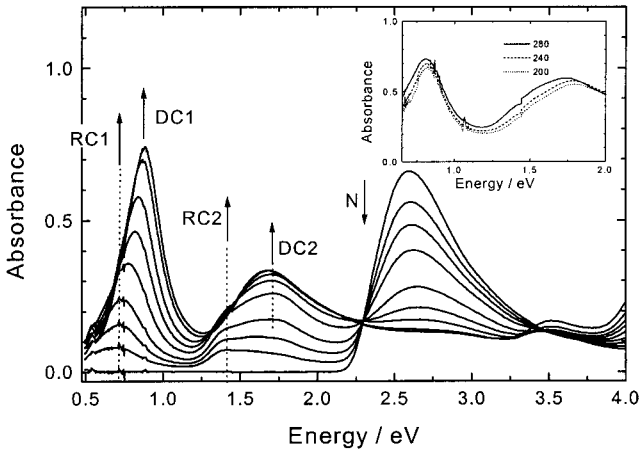

Figure 7. UV/visible/near-IR spectra of **G3-11T-G3** as a function of the doping level by the stepwise addition of 2 equiv of $THIClO_4$ recorded in a 10 mm cell. The graph shows the formation of cation radicals (RC1 and RC2) at the expense of neutral molecules (N) and the subsequent conversion to dications. The inset shows the variation of the spectrum with temperature in the range from 280 to 200 K.

a disproportionation equilibrium of two monocation radicals into a neutral and doubly charged oligomer is operative for these long oligothiophenes, the hypsochromic shift of the spectrum can be rationalized in two ways. First, a quadruply charged spinless π-dimer could be formed in which each molecule carries two noninteracting charges.[38] The second possibility is that the dicationic state of these lengthy oligothiophenes is a singlet state (i.e. spinless) carrying two individual polarons.[34] Such behavior has been predicted based on theoretical calculations[41] and can be qualitatively rationalized by the decrease in Coulomb repulsion that is obtained upon moving the positive polarons further apart, which, at certain length, outweighs the energy cost required for creating two polaronic deformations vs a single bipolaronic structure. In accordance with this proposition, the bands of the **G3-11T-G3**$^{2+}$ dication (0.89 and 1.68 eV, $n = 11$) are found at almost the same position as those of the **Ph-5T-B**$^{+\bullet}$ cation radical (0.93 and 1.66 eV, $n \approx 5.5$) which has half the effective conjugation length.

Cyclic voltammetry of the two 17T derivatives in solution only produced very low currents that could not be analyzed. Therefore, **B-17T-B** and **G3-17T-G3** were investigated as drop-cast films deposited on the Pt electrode and cyclic voltammograms were recorded in CH_3CN to prevent their dissolution (a similar procedure is often employed for poly(alkylthiophenes)).[42] The cyclic voltammogram of a thin film of **B-17T-B** shows a large difference of 210−225 mV between anodic and cathodic peak currents (Figure 3, Table 1). For **G3-17T-G3** the splitting is even larger amounting to 300 mV. The anodic peak currents of **B-17T-B** and **G3-17T-G3** scale linearly with the scan rate in the range of 25 to 200 mV/s, as expected for a thin solid film on the electrode. In both films, the reversal peak of the discharging is shifted to lower energy compared to the original oxidation peak. The same behavior has been observed for short-chain oligothiophenes and oligophenylenes in the solid state but

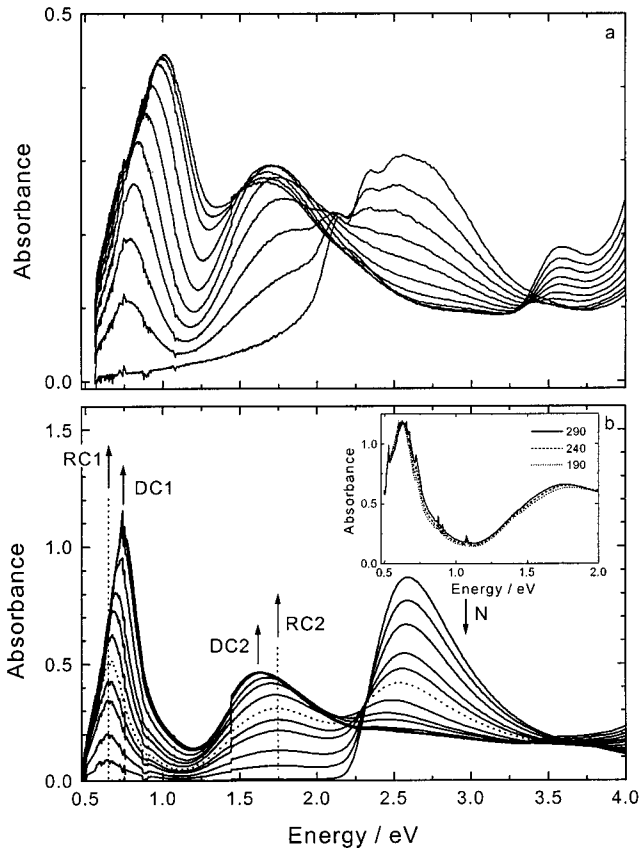

Figure 8. UV/visible/near-IR spectra of (a) **B-17T-B** and (b) **G3-17T-G3** as a function of the doping level by the stepwise addition of 2 equiv of $THIClO_4$ recorded in a 10 mm cell. Graph b shows the formation of cation radicals (RC1 and RC2) at the expense of neutral molecules (N) and the subsequent conversion to dications. The inset of graph b shows the variation of the spectrum with temperature in the range from 290 to 190 K.

not in solution.[43,44] The explanation for this behavior postulated by Meerholz and Heinze involves a two-step process during the charging of the oligomer films:[43,44] first the molecules stabilize themselves from an originally twisted conformation into a more planar, quinoid-like structure with enhanced π-conjugation, thus resulting in discharge at potentials of lower energy. The second step involves an intermolecular stabilization through interactions between neighboring charged segments, thus leading to increased delocalization and further stabilization.

The UV/visible/near-IR spectra of **B-17T-B** and **G3-17T-G3** as a function of doping level are shown in Figure 8. The solubility of **B-17T-B** in CH_2Cl_2 is limited and the spectrum of the neutral compound in Figure 8a reveals that the oligomer is in an aggregated state even under these conditions. The broad onset of the $\pi-\pi^*$ absorption and the appearance of resolved vibronic fine structure in the absorption band are characteristic of a system that is not molecularly dissolved. During the oxidation two transitions are observed that shift to lower and higher energy with increased doping level. The **G3-17T-G3** oligomer dissolves molecularly and thus can be analyzed in much more detail as a result of the solubilizing effect of the G3 dendrons. The UV/visible/near-IR spectra of the oxidation process are shown in Figure 8b. The spectrum recorded after addition of the first aliquot of $THIClO_4$ shows two transitions

(40) In fact the temperature independence only shows that the π-dimerization equilibrium does not shift in the temperature range. In principle this does not imply that π-dimers are absent, since a similar result could have been obtained when all cation radicals are present as π-dimers, even at the highest temperature.

(41) (a) Tol, A. J. W. *Chem. Phys.* **1996**, *208*, 73. (b) Tol, A. J. W. *Synth. Met.* **1995**, *74*, 95.

(42) Zagorska, M.; Pron, A.; Lefrant, S. In *Handbook of Organic Conductive Molecules and Polymers*; Nalwa, H. S., Ed.; Wiley: New York, 1997; Vol. 3, Chapter 4, p 183.

(43) Meerholz, K.; Heinze, J. *Electrochim. Acta* **1996**, *41*, 1839.

(44) Meerholz, K.; Heinze, J. *Angew. Chem., Int. Ed. Engl.* **1990**, *29*, 692.

(45) Apperloo, J. J.; Malenfant P. R. L. Unpublished results.

with peaks at 0.66 and 1.74 eV (Figure 8b). As anticipated, the first transition occurs at a position slightly lower in energy than the RC1 band of **G3-11T-G3**$^{+\bullet}$ (0.69 eV, Table 2), but the second transition is unexpectedly at a much higher energy (1.74 vs 1.42 eV, Table 2). A more critical look at the spectra shown in Figure 7 and Figure 8b reveals that the low-energy onset of the RC2 band for both **G3-11T-G3**$^{+\bullet}$ and **G3-17T-G3**$^{+\bullet}$ is at ~1.25 eV. The relatively higher energy of the RC2 peak of **G3-17T-G3**$^{+\bullet}$ is probably the result of an increased contribution of the 0−1 or 0−2 vibronic transitions to the absorption band. In this respect it should also be mentioned that the maximum of the RC2 band of **G3-11T-G3**$^{+\bullet}$ is not at a constant value but shifts from 1.42, to 1.61, and finally to 1.70 eV during the first three oxidation steps (Figure 7). Such changes do not occur for **G3-17T-G3** for which at least the first five to six spectra have the same RC2 peak energies. However, beyond this point, a change in the spectra occurs and the low-energy RC1 band exhibits a hypsochromic shift whereas the high-energy RC2 band exhibits a bathochromic shift. Variable-temperature UV/visible/near-IR spectra recorded at the oxidation level where this transition occurs reveal that the spectrum is temperature independent in the range from 290 to 190 K. As was the case for **G3-11T-G3**$^{+\bullet}$**,** this demonstrates that no change in the π-dimerization equilibrium occurs for **G3-17T-G3**$^{+\bullet}$ in this temperature range.[40] Furthermore, the bands of the **G3-17T-G3**$^{2+}$ dication (0.75 and 1.62 eV, $n = 17$) are found at almost the same position as those of a cation radical possessing half the conjugation length (i.e. **8T-B**$^{+\bullet}$ bands are found at 0.71 and 1.49 eV, $n = 8$[43]). This behavior is analogous to that of the **G3-11T-G3**$^{2+}$ dication and corroborates the view that long oligothiophenes accommodate two polarons on a single chain in their doubly oxidized state.[34]

Conclusions

We have shown that dendrimers consisting of oligothiophene cores and poly(benzyl ether) dendrons can be converted into stable cation radicals and dications by chemical oxidation, depending on the oligomer length and the dendron generation. The first generation (G1) dendritic end groups are effective in stabilizing the reactive 4T$^{+\bullet}$ cation radical against α-coupling. For the higher generation end groups (G2 and G3) the stabilization of 4T$^{+\bullet}$ is less effective. The decreased stabilization for higher generations is tentatively attributed to an intramolecular redox reaction of the back-folded dendritic wedges with the rather localized charge of 4T$^{+\bullet}$. The cation radicals of the longer oligothiophenes ($n = 5$, 9, 11, and 17) functionalized with dendritic wedges (including those with **G3** substitution) have a lower oxidation potential (Table 1) and are intrinsically more stable as a result of the increased delocalization of charge and electron spin. The electronic transitions of the cation radical and dication of these novel hybrid systems follow an approximate linear relation with the reciprocal conjugation length, in agreement with observations for other oligothiophenes.[20,21] These results demonstrate that, apart form the shortest cation radicals ($n = 4$), the principal electroactive properties of the oligothiophenes are not affected by the poly(benzyl ether) dendritic wedges, thus presenting an interesting option for combining optoelectronic properties, processability, and dimensional order in thin films and aggregates. Some clear "dendrimer-related" effects could be established such as the electrochemical oxidation being kinetically limited when the dendrons are large in comparison to the electrophore. Furthermore, variable-temperature experiments on the **Ph-5T-G3**$^{+\bullet}$ cation radical revealed that π-dimerization is not inhibited by the dendritic wedges, yet the dimerization enthalpy is reduced. Furthermore, the low-temperature studies of **Ph-5T-G3**$^{+\bullet}$ cation radicals constitute the first example in which a supramolecular dendritic assembly results from the π-dimerization of oxidized oligomers. Last, with the chemical oxidation of **G3-17T-G3**$^{+\bullet}$ and **G3-17T-G3**$^{2+}$, we have characterized the longest well-defined oligothiophene cation radical and dication to date. We find that the electronic transitions of the doubly oxidized state of the lengthy oligothiophenes **G3-11T-G3** and **G3-17T-G3** are consistent with the view that they carry two independent polarons rather than one bipolaronic deformation, which is formed for oligomeric dications with up to nine thiophene units such as **9T-(B)** and **9T-(G*2)**.[34] The rationale for this transition, which occurs at about 10 thiophene units in oligothiophene dications, is that the decrease in Coulomb repulsion which is obtained by moving the two positive charges further apart along the chain outweighs the energy cost required for creating two individual geometry deformations on the chain, instead of a single deformation associated with a bipolaron. Further studies on the supramolecular aggregation of neutral chains in solution and thin films are currently underway.

Acknowledgment. We would like to thank Prof. E. W. Meijer (TUE) for stimulating discussions and advice. This research has been supported by The Netherlands Organization for Chemical Research (CW), The Netherlands Organization for Scientific Research (NWO) through a grant in the PIONIER program (J.J.A., R.A.J.J.), the Air Force Office of Scientific Research through their MURI program, and the National Science Foundation NSF-DMR No. 9816166 (P.R.L.M., J.M.J.F.). The preparation of the G3 dendron by Stefan Hecht (Berkeley) is also acknowledged.

Supporting Information Available: Experimental details pertaining to the synthesis and characterization of novel compounds (PDF). This material is available free of charge via the Internet at http://pubs.acs.org.

JA994259X